Optimal Control Allocation with Load Sensor Feedback for Active Load Suppression, Flight-Test Performance

Christopher J. Miller[1] and Dan Goodrick[2]
NASA Neil A. Armstrong Flight Research Center, Edwards, CA, 93523

The problem of control command and maneuver induced structural loads is an important aspect of any control system design. The aircraft structure and the control architecture must be designed to achieve desired piloted control responses while limiting the imparted structural loads. The classical approach is to utilize high structural margins, restrict control surface commands to a limited set of analyzed combinations, and train pilots to follow procedural maneuvering limitations. With recent advances in structural sensing and the continued desire to improve safety and vehicle fuel efficiency, it is both possible and desirable to develop control architectures that enable lighter vehicle weights while maintaining and improving protection against structural damage. An optimal control technique has been explored and shown to achieve desirable vehicle control performance while limiting sensed structural loads to specified values. This technique has been implemented and flown on the National Aeronautics and Space Administration Full-scale Advanced Systems Testbed aircraft. The flight tests illustrate that the approach achieves the desired performance and show promising potential benefits. The flights also uncovered some important issues that will need to be addressed for production application.

Nomenclature

A	=	state derivative coefficients
Aero	=	aerodynamic
ARTS IV	=	Airborne Research Test System four
B	=	control effectiveness matrix
CAT	=	choose a test
DAG	=	dial a gain
FAST	=	Full-scale Advanced Systems Testbed
FC	=	flight condition
FDMS	=	Flight Defection Measurement System
fbk	=	feedback
filt	=	filtered
g	=	acceleration of gravity
H	=	trim tuning matrix
HM	=	hinge moment
I	=	inertia tensor
ITB	=	integrated test block
KCAS	=	knots calibrated airspeed
J	=	cost function value
K	=	roll mode gain
L	=	matrix of surface influence coefficients for each measured load
LOES	=	low order equivalent systems

[1] Full-Scale Advanced Systems Testbed Chief Engineer, Flight Controls and Dynamics, P.O. Box 273 Edwards, California/MS 4840D, AIAA Member.
[2] Research Engineer, Instrumentation Branch, P.O. Box 273 Edwards, California/MS 4800-1409, AIAA Member.

M	=	measured loads vector
N	=	load cost function simplification parameter
NDI	=	Nonlinear Dynamic Inversion
NWS	=	nose wheel steering switch
n	=	load constraint steepness
OCLA	=	Optimal Control and Load Allocation
PI	=	proportional plus integral
PSD	=	power spectral density
p	=	roll rate
psf	=	pounds per square foot
q_c	=	impact pressure
ref	=	reference
RFCS	=	research flight control system
S	=	aerodynamic reference area
SMI	=	structural modal interaction
s	=	Laplace operator
u	=	control surface vector (m-measured, p-trim)
x	=	state vector
γ	=	load constraint weight
ε	=	trim cost weight
ζ	=	damping ratio
ω	=	angular velocity vector
ω_n	=	roll mode natural frequency

Superscripts

$\rightarrow$	=	vector quantity
$\cdot$	=	time derivative
b	=	body fixed axis
e	=	earth fixed axis

I. Introduction

CURRENT control applications account for structural load limits by: limiting the types of control algorithms that can be applied to a given application, requiring additional structural margin resulting in less efficient designs, and placing procedurally enforced restrictions on pilot control actions and maneuvers. One possible technology that may alleviate some of these constraints is to utilize structural sensing feedback to actively sense and limit critical loads. A number of theoretical and simulation studies[1-3] have been published on this topic, but a flight experiment is essential to evaluate the feasibility and applicability of the approach. This technology would facilitate lighter weight optimized structure, increase robustness of the system to off nominal and unpredicted situations (stall/spin, accidental damage), and pave the way for highly optimized high performance control algorithms with less deterministic structural interaction.

The specific goal for this experiment is to explore the merits of Optimal Control Allocation[3] with structural feedback in flight. Experimental testing on a full-scale piloted vehicle will provide valuable insight into the performance of the technique in a flight environment and help explore potential handling qualities issues with the approach. The experiment was conducted on the Full-scale Advanced Systems Testbed (FAST) in part because of the research instrumentation system on the aircraft. The measured aileron hinge moment was the selected critical load for this experiment. The goal of the experiment is to maintain the roll performance of the aircraft while actively enforcing load limits on the ailerons.

II. Problem Statement and Research Objectives

The current design paradigm for flight controls and vehicle structures has worked extremely well, and resulted in exceptional levels of safety and performance. However, as American Airlines Flight 587 (Fig. 1) illustrates, there are limits to the existing design approach.[4] Flight 587 encountered the wake of a larger transport, the result of which

violently upset the airplane. The pilot, acting consistent with his vehicle upset training, attempted to recover control with the aggressive use of the rudder pedals. The combination of maneuver and rudder induced loads broke the vertical tail off, resulting in complete loss of control. All of this activity occurred below the published maneuvering speed of the airplane which had been incorrectly understood as a safe speed for rapid and aggressive rudder pedal inputs. This incident provides a sobering illustration of the possible benefits of a control architecture that protects aircraft structure while using all available control effectors to provide the pilot with the necessary control response. Future aircraft with load limiting control technologies could give the pilot the best possible control response in an emergency while minimizing the threats posed by control and maneuver induced catastrophic structural failure.

Figure 1. American Airlines Flight 587.

The Optimal Control and Load Allocator (OCLA) experiment was designed to test the effectiveness and robustness of an optimal control allocator with strain-gauge feedback at limiting aircraft loads while producing the desired aircraft response commanded by the pilot. The OCLA experiment is built on top of the Nonlinear Dynamic Inversion (NDI)[5,6] baseline controller utilized by previous experiments flown on the FAST aircraft. Specifically, the experiment is designed to limit the measured aileron hinge moment on the National Aeronautics and Space Administration (NASA) FAST while maintaining desired handling qualities for an air-to-air tracking task. The following is a list of the detailed experiment objectives.

Objective 1: Limit the aileron motion subject to a defined load constraint.
Metric: The measured aileron hinge moment does not exceed 100% of the specified value for any of the test scenarios.

Objective 2: Maintain the roll performance of the original controller that does not utilize structural load as a constraint.
Metric: No worse than a 10% reduction in the roll mode time constant or the steady state roll rate for up to half roll stick maneuvers.

Objective 3: Maintain the handling qualities ratings of the original controller that does not utilize structural load as a constraint.
Metric: No worse than one Cooper-Harper[7] rating degradation for the tasks with aileron motion clipping due to the load constraint.

III. Scope and Technical Approach

The NASA Armstrong FAST was used as an in-flight laboratory to demonstrate the technical feasibility of load limiting control via optimal control allocation. The testbed aircraft and the research envelope have been specifically designed to facilitate rapid prototyping of advanced control and sensor technologies.[8] Within the limited research envelope (Fig. 2), a wide array of sensor technologies and control schemes can be evaluated in flight with minimal testing between design iterations. This envelope is commonly referred to in other FAST related publications as the Class B envelope.

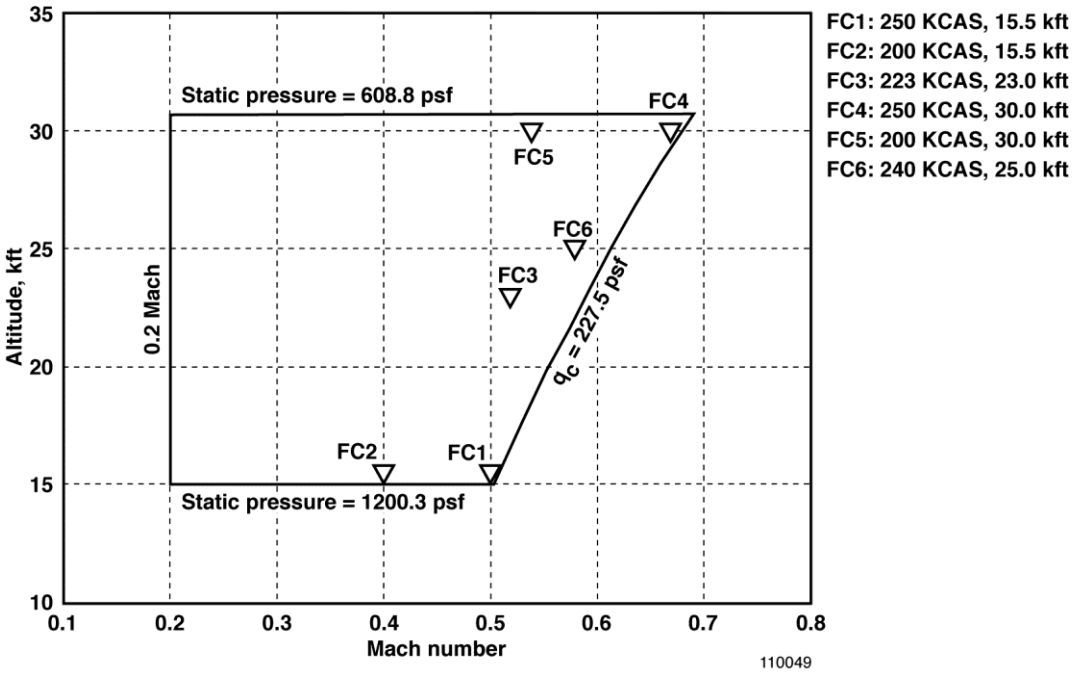

Figure 2. Research envelope (Class B).

The OCLA experiment used the outputs from four foil strain bridges as feedbacks, two redundant bridges on each aileron. The redundant sensors were compared to the primary strain gauges to mitigate concerns about failure of research instrumentation used as feedback in a control law. When the strain gauges were installed they were not intended as primary flight control feedback parameters and as such are not as reliable as would be desired for a production representative design. These measured strains on the aileron control arms were used to calculate the actual hinge moments on each aileron. Excessive hinge moments can cause premature fatigue and failure of the ailerons and the surrounding structure. Conceptually, the experiment is designed to illustrate that the optimal allocator will actively limit the measured aileron hinge moments and reallocate the pilot commanded body rates to other control surfaces such as the trailing-edge flaps and the stabilators, thereby, sensing and limiting the imparted aileron loads while still giving the pilot the desired vehicle response.

Due to the low dynamic pressures achievable in the Class B envelope, it is not possible to achieve aileron hinge moments approaching the actual limit for the ailerons; therefore, it is necessary to set an arbitrarily low target limit to test out the algorithm. This reduced limit was tunable in flight and was based on the largest hinge moment measured during past experiments within the Class B envelope of 15000 in-lb.

IV. Experimental Control Law Description

The control laws under test for the flights covered by this paper are described in detail in Ref. 9. Figure 3 is a top level block diagram of the control laws. The control laws are made up of reference models for handling qualities, a proportional plus integral compensator for robustness, and a control surface allocation scheme that optimizes a cost function. The cost function (Fig. 4) is made of up three elements: the first is based on dynamic inversion to achieve

desired command tracking, the second is an element that drives the control surfaces to defined trim positions, and the last is an element that utilizes load feedback and prevents structural overload. The cost function and each of the parameters contained in it are shown in Fig. 4.

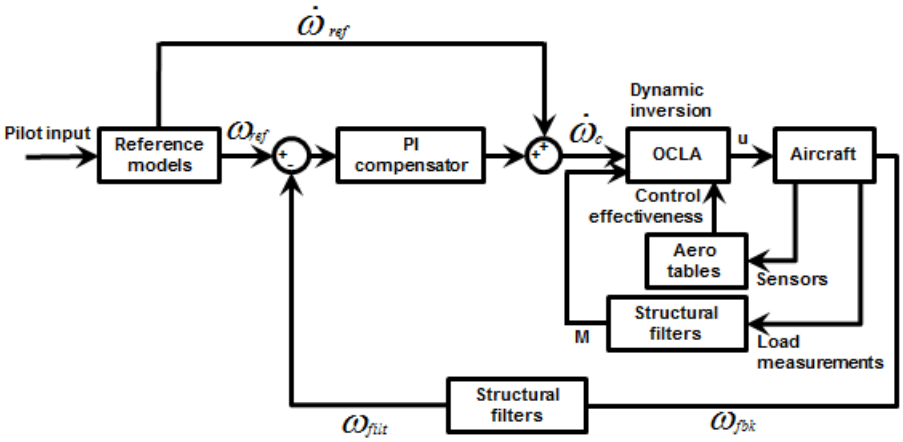

Figure 3. Control law block diagrams.

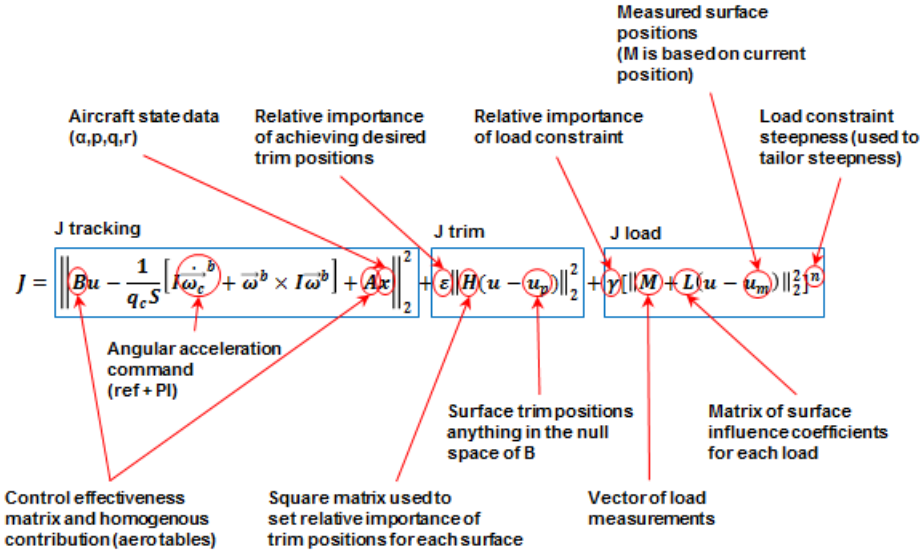

Figure 4. Cost function description.

V. Aircraft Description

The FAST vehicle is primarily a flight controls research platform, and as such is largely architected around the aircraft flight control computers, as shown in Fig. 5. The production flight control computers have been modified with an additional processor in each channel to accommodate a research flight control system (RFCS). In order to provide even greater computational and interface capabilities, the RFCS has been augmented with two identical external airborne research test system (ARTS IV) computers. Experimental software housed within the RFCS and ARTS IV computers can exercise full control over the aircraft flight control surfaces as well as the engine throttle levers.

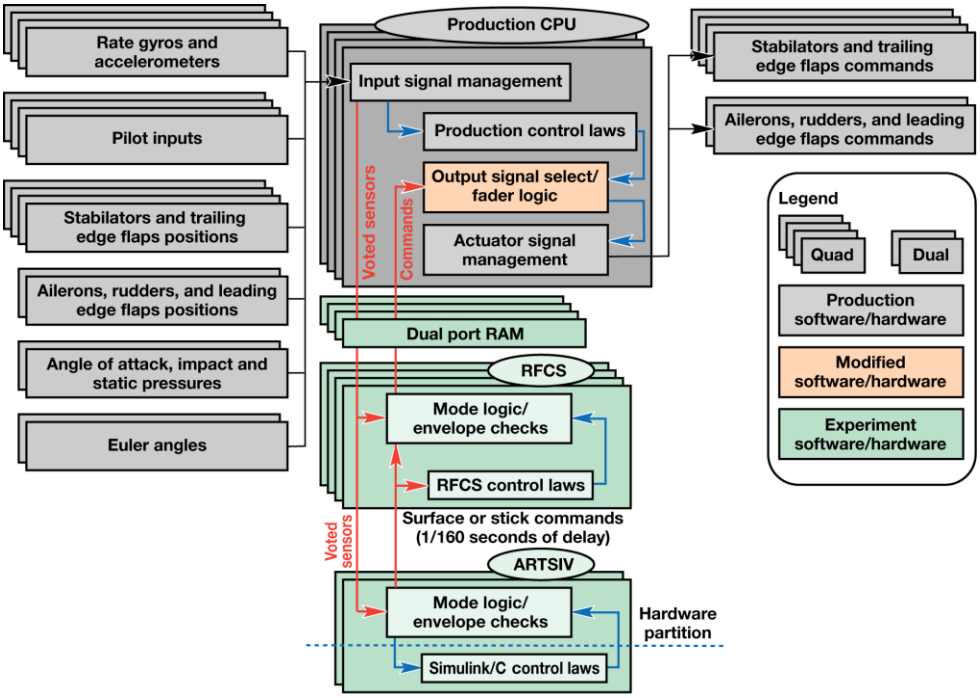

Figure 5. FAST systems overview.

In addition to its research flight control capabilities, the FAST testbed has been outfitted with extensive research instrumentation. Loads, dynamics, and aerodynamic parameters as well as data from the production flight control systems and on-board experiments are recorded onboard the aircraft and telemetered to the ground for real-time control room monitoring and post-flight data analysis.

Pilot interfaces are provided for situational awareness, experiment selection and configuration, and to facilitate transitions between the production and research flight control systems. Flight control authority automatically reverts to the production control system in the event of a system failure or when a flight envelope constraint is violated.

VI. Flight-Test Approach

The following sections describe the flight-test approach including the test envelope and the experimental configurations explored. The flight-test maneuvers and their associated objectives are also described.

A. Flight Envelope

Figure 2 shows the FAST Class B envelope. All of the OCLA test maneuvers were performed in the class B envelope. Flight Condition (FC) 6 was the primary test point for all of the test maneuvers including the starting flight condition for the handling qualities tests. FC6 was chosen as the primary test point because it allowed sufficient margin away from the envelope limits for the pilots to use for maneuvering. Additionally, FC11 was used to show that the control law is not a point design and to show that there were no handling qualities cliffs at the slower speed. This low speed test gave the pilot more airspeed margin when performing the handling qualities tasks.

B. Experimental Configurations

Each experiment can be configured prior to engagement through the use of two independent configure numbers which are referred to as dial-a-gain (DAG) and choose-a-test (CAT). A full set of valid DAG-CAT combinations can be found in Table 1. Further description of the experiment configuration parameters can be found in Ref. 9.

In addition the to the DAG-CAT configurations, the nose wheel steering switch (NWS) is used once the experiment is engaged to set the desired level of the aileron hinge-moment limit for the experiment. Each successive button press results in a more restrictive limit until the lowest limit is reached at which time the counter resets. The hinge-moment limits and their associated NWS count are shown in Table 2.

Table 1. OCLA DAG and CAT configuration table.

DAG	CAT	Trim penalty weight (ε)	Load constraint exponent (n)	Strain filtering on/off	Allocation scheme
22	14-21	N/A	N/A	N/A	Weighted pseudo inverse (Classic NDI)
23	14	0.0001	20	Off	Optimal control allocation with load constraint
23	15	0.001	20	Off	Optimal control allocation with load constraint
23	16	0.005	20	Off	Optimal control allocation with load constraint
23	17	0.01	20	Off	Optimal control allocation with load constraint
23	18	0.0001	20	On	Optimal control allocation with load constraint
23	19	0.001	20	On	Optimal control allocation with load constraint
23	20	0.005	20	On	Optimal control allocation with load constraint
23	21	0.01	20	On	Optimal control allocation with load constraint
24	14	0.0001	10	Off	Optimal Control Allocation with Load Constraint
24	15	0.001	10	Off	Optimal control allocation with load constraint
24	16	0.005	10	Off	Optimal control allocation with load constraint
24	17	0.01	10	Off	Optimal control allocation with load constraint
24	18	0.0001	10	On	Optimal control allocation with load constraint
24	19	0.001	10	On	Optimal control allocation with load constraint
24	20	0.005	10	On	Optimal control allocation with load constraint
24	21	0.01	10	On	Optimal control allocation with load constraint
25	14	0.0001	4	Off	Optimal control allocation with load constraint
25	15	0.001	4	Off	Optimal control allocation with load constraint
25	16	0.005	4	Off	Optimal control allocation with load constraint
25	17	0.01	4	Off	Optimal control allocation with load constraint
25	18	0.0001	4	On	Optimal control allocation with load constraint
25	19	0.001	4	On	Optimal control allocation with load constraint
25	20	0.005	4	On	Optimal control allocation with load constraint
25	21	0.01	4	On	Optimal control allocation with load constraint

Table 2. Aileron hinge-moment limits versus NWS counter.

NWS: 0	load limiting off
NWS: 1	16,000 in-lb
NWS: 2	12,000 in-lb
NWS: 3	10,000 in-lb
NWS: 4	7,000 in-lb
NWS: 5	5,000 in-lb

C. Flight-Test Maneuvers

Comparisons of the aircraft dynamics and control surface usage with and without load limiting engaged are used to quantify the benefits and drawbacks of the load liming optimal control allocator. Table 3 shows the test blocks used and their traceability to the experiment objectives.

Table 3. Flight-test block descriptions.

Test block	Test block description	Objective 1 (Load limiting)	Objective 2 (Roll frequency response)	Objective 3 (Handling Qualities)
A	Integrated test block (ITB)	☑	☑	
B	Frequency sweeps	☑	☑	
C	2-g air-to-air tracking	☑		☑

The test blocks are structured such that they are build-up for each other. In other words, Test Blocks A and B are accomplished first and are used to show that Test Block C is safe to execute. Test Block A consists of basic aircraft maneuvers used to progressively expand the envelope with maneuvers with increasing magnitude and complexity. The maneuvers in Test Block A are executed in order as follows:

1) Pitch, roll, and yaw doublets
2) 360 degree rolls left and right (up to full stick)
3) 2-g rolling pull out (left or right)
4) 2.5-g level turn (left or right)

Once the control laws have been shown to have acceptable characteristics using Test Blocks A and B, the handling qualities tasks in Test Block C can be executed.

The handling qualities task used for this experiment was a 2-g tracking task broken up into gross acquisition and fine tracking sub tasks. For the gross acquisition task the target aircraft starts line abreast with the test aircraft at ~0.5 miles separation. Then at the direction of the test aircraft pilot the target aircraft initiates a 2-g level turn, and the test aircraft aggressively attempts to place the target aircraft within a targeting reticle. The desired performance criteria for the gross acquisition task is to place the target inside the reticle with no overshoots, and adequate criteria is with no more than one overshoot. The fine tracking task begins once the gross acquisition task is completed, and the test aircraft pilot instructs the target aircraft to begin gentle roll maneuvers. While the target aircraft is maneuvering, the test aircraft pilot attempts to keep the pipper in the center of the targeting reticle on the target aircraft. Desired tracking criteria for the fine tracking task is keeping the pipper on target 80% of the time, and adequate tracking criteria is keeping the pipper on target 50% of the time.

VII. Flight Results

The following sections highlight the flight results for all of the objectives. The results discuss both positive and negative outcomes from the relatively small flight-test campaign.

A. Effectiveness of OCLA at Hinge-Moment Limiting (Objective 1)

Figure 6 illustrates that during a 360° roll maneuver that the algorithm with load limiting activated provided the desired hinge-moment limiting. It can also be seen in Fig. 6 that the same steady state roll rate was achieved, but that the onset rate for the more restrictive limit was reduced as expected. Figure 7 shows that during the maneuver with the more restrictive load limit, the roll command utilized less differential aileron, as expected, and that more differential trailing-edge flaps and differential stabilators are used instead to achieve the desired roll performance. An adverse SMI interaction can be seen on the hinge-moment measurement in Fig. 6 with the restrictive limit. This structural modal interaction is a result of insufficient notch filtering on the strain-feedback parameters. This behavior will be discussed in more detail in section D. Figure 8 shows the variation of the cost function values during the roll maneuver. The value of the cost related to the tracking constraint is adversely affected by the more restrictive hinge-moment limit. This result is expected because with more restrictive hinge-moment limits the controller has to sacrifice tracking performance to maintain the load limits.

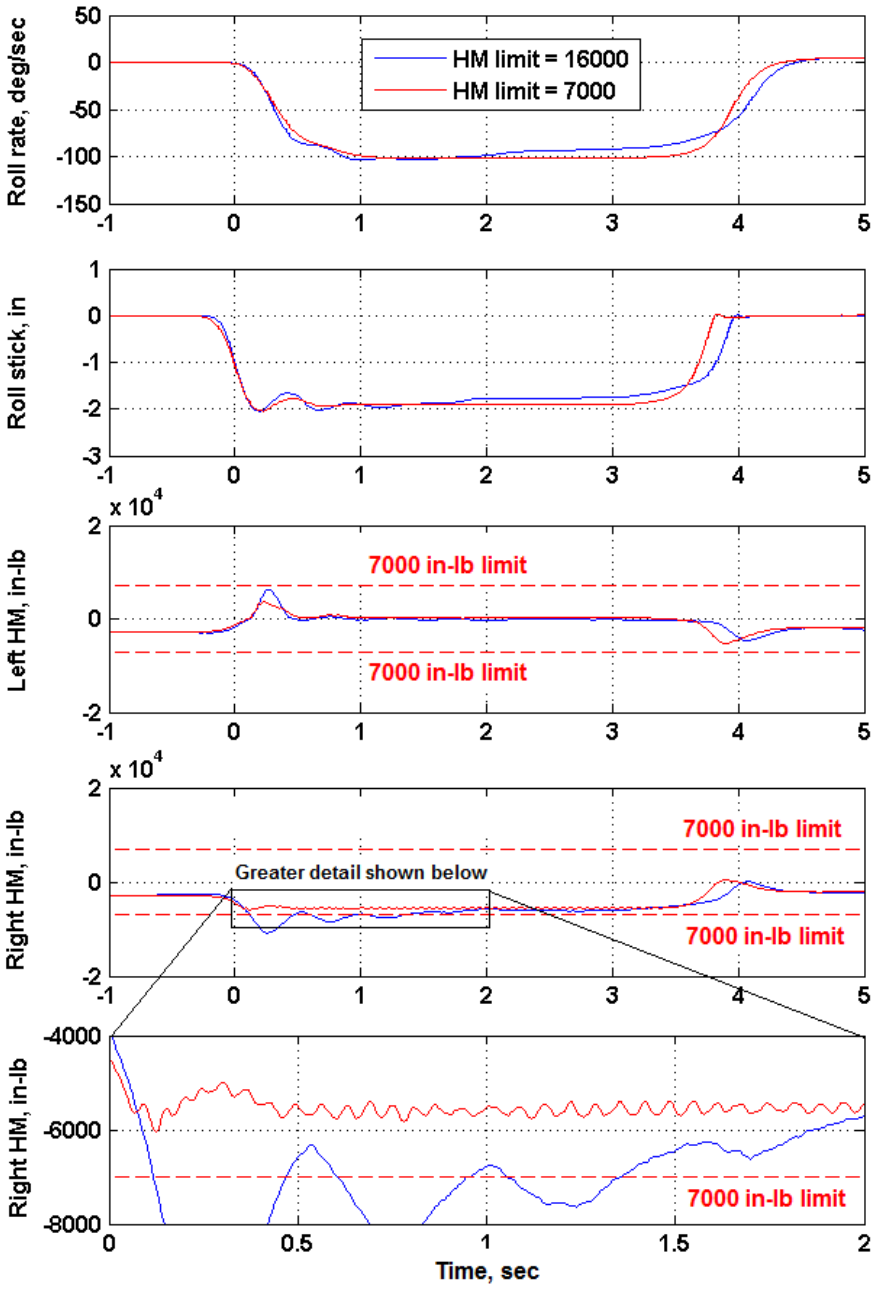

Figure 6. Illustration of OCLA performance during a 360º roll with 65% roll stick (FC6).

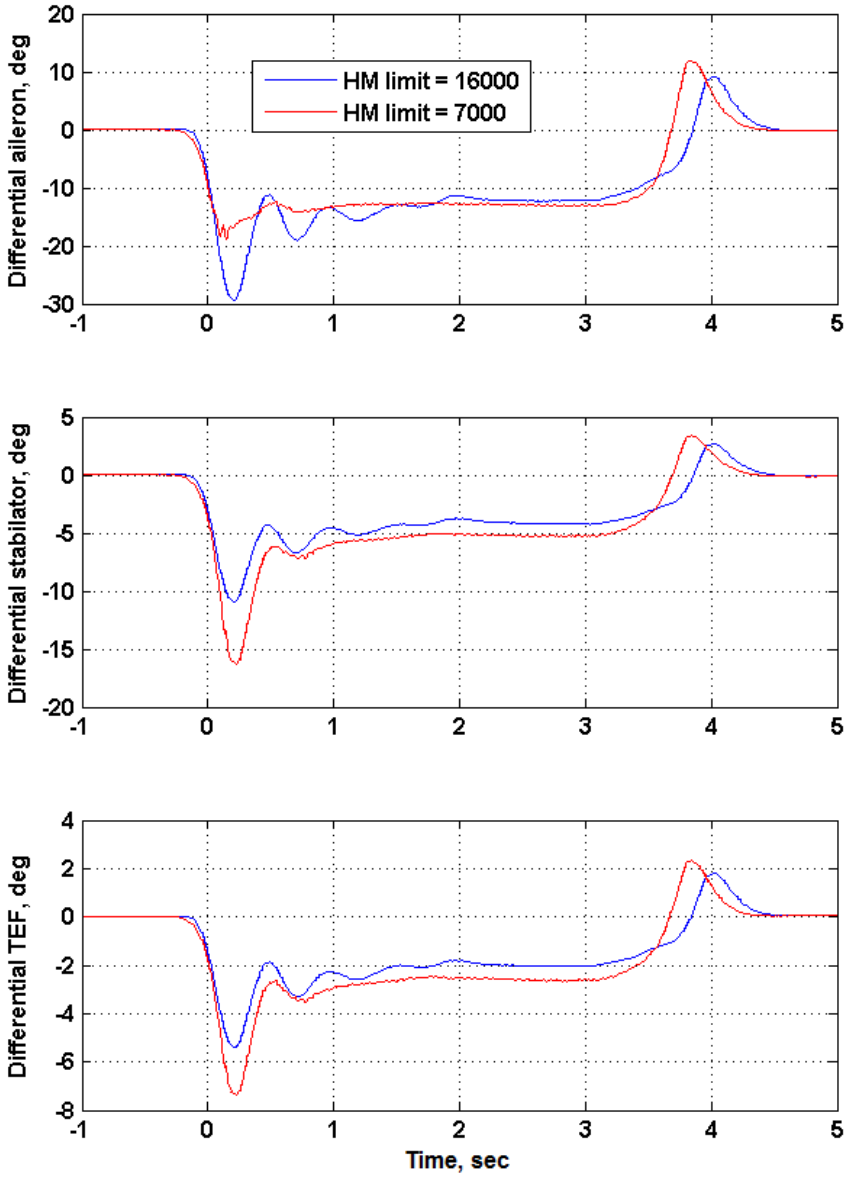

Figure 7. Control surface usage during 360° roll with 65% roll stick (FC6).

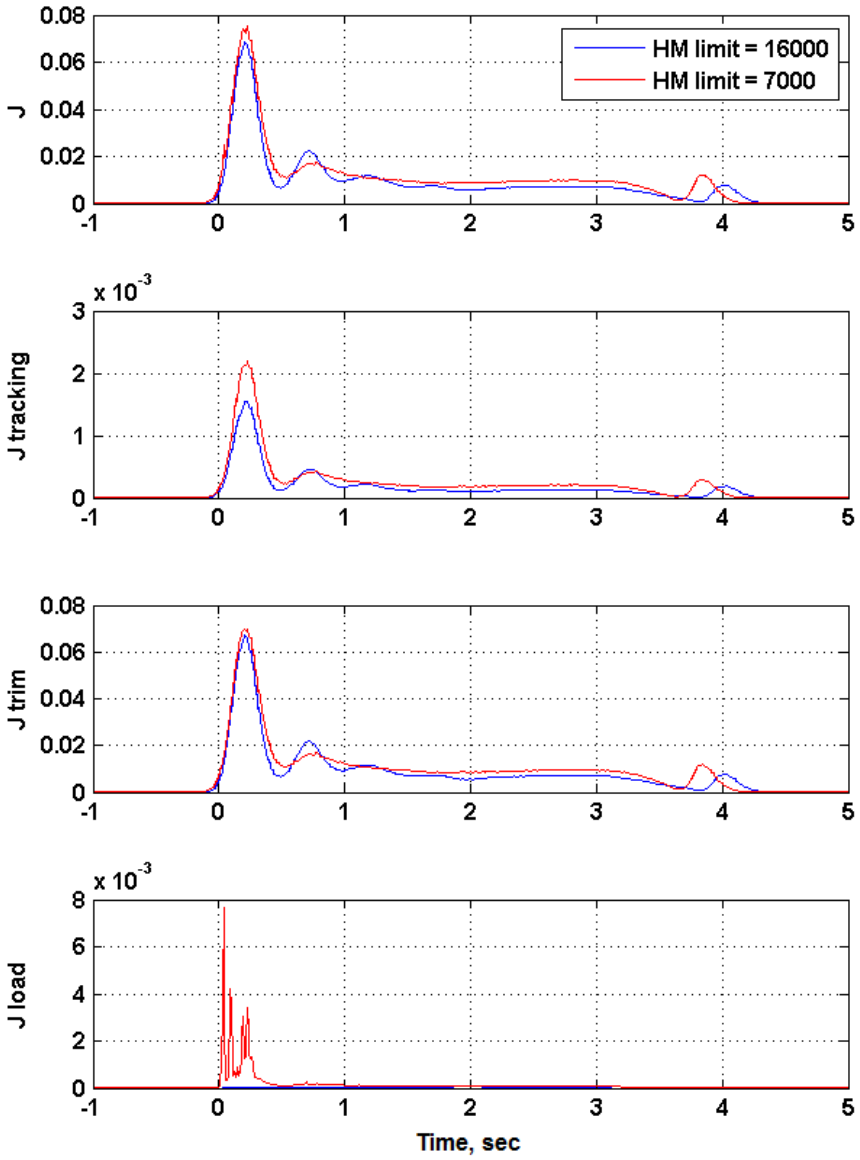

Figure 8. Cost function variation during 360° roll with 65% roll stick (FC6).

Figure 9 illustrates the controller performance during a 2.5-g level turn at FC6. It can be seen that when configured to do so the hinge moment is limited to below the 7000 in-lb limit by fairing both ailerons symmetrically up (negative direction) to reduce load. However, there is a little oscillatory behavior on both hinge-moment measurements and the symmetric aileron command for the 7000 in-lb hinge-moment limit. These oscillations are related to the excitation of a structural mode at high angle of attack due to separated flow and the associated buffet on the aileron and wing. Also it can be seen that the steady state aileron hinge moment is not as close to the 7000 in-lb limit as desired. The load constraint appears to start to activate when the load is at about 65% of the limit instead of the 80% target that the weights were tuned to achieve. This reduction in steady state hinge moment is due to the fact that multiple measurements are nearing their limit instead of just one. This early activation of the load constraint reduces the amount

of aileron command available for command tracking, thus reducing aircraft performance. This reduction in performance suggests that further shaping of load measurements beyond just the load constraint exponent may be desirable.

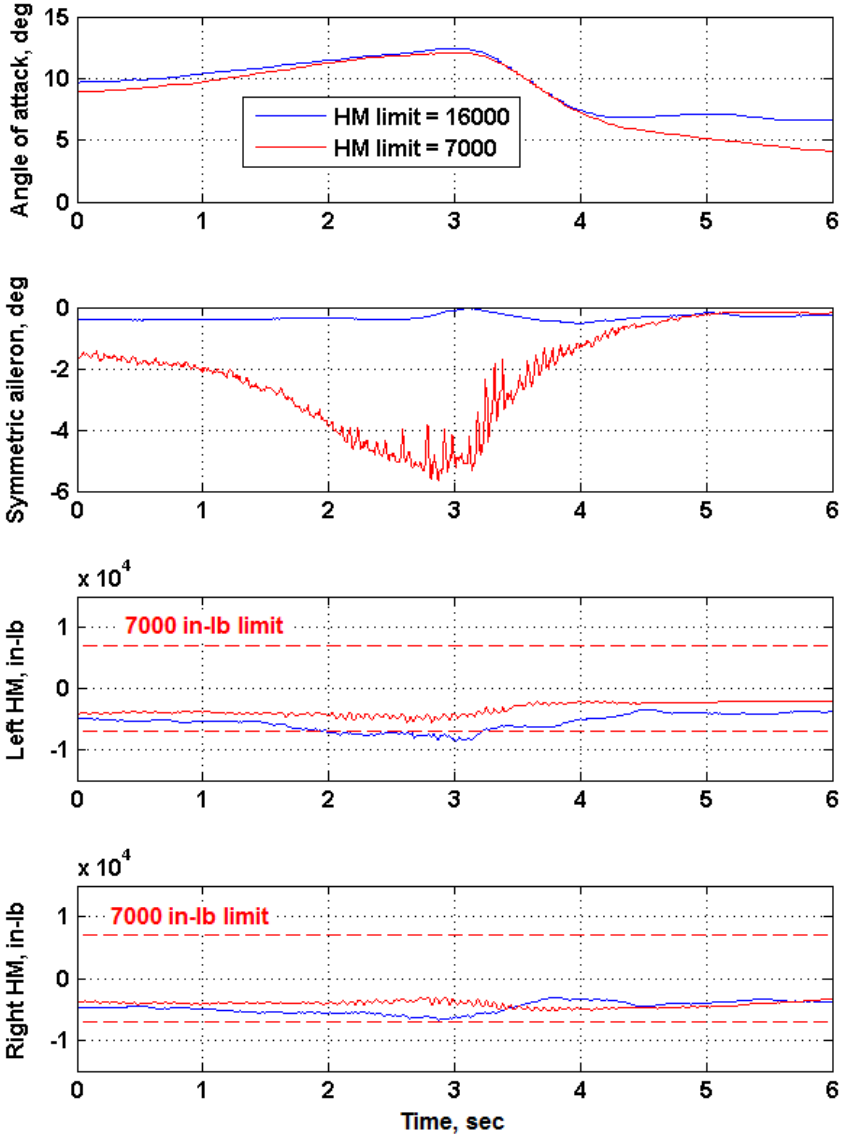

Figure 9. Performance during a 2.5-g level turn (FC6).

Figures 10 and 11 show the behavior of the cost function for this same level turn maneuver. The load constraint being active appears to increase the number of iterations required for the optimization to converge as was predicted by the simulation results in Ref. 9. The results in Figs. 10 and 11 also appear to show that the minimization of the load constraint tends to increase the tracking error and trim aspects of the cost function.

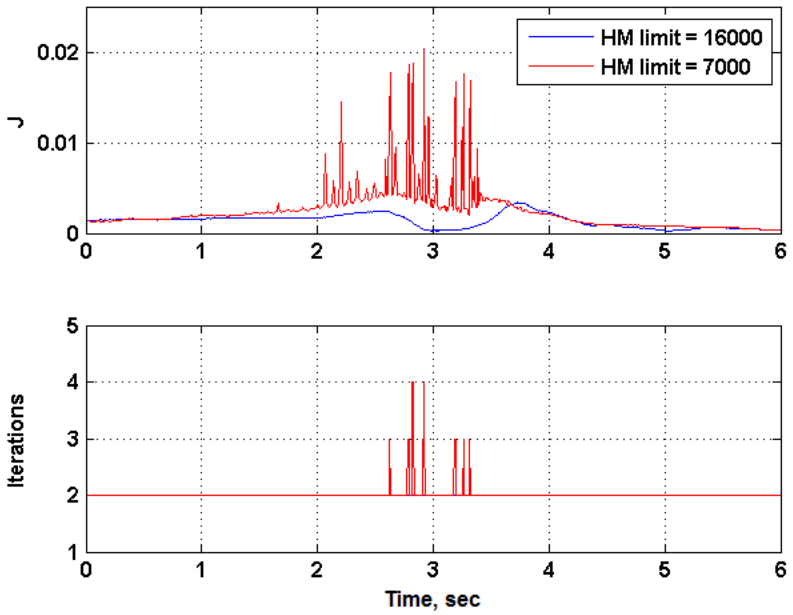

Figure 10. Cost and number of iterations during a 2.5-g level turn (FC6).

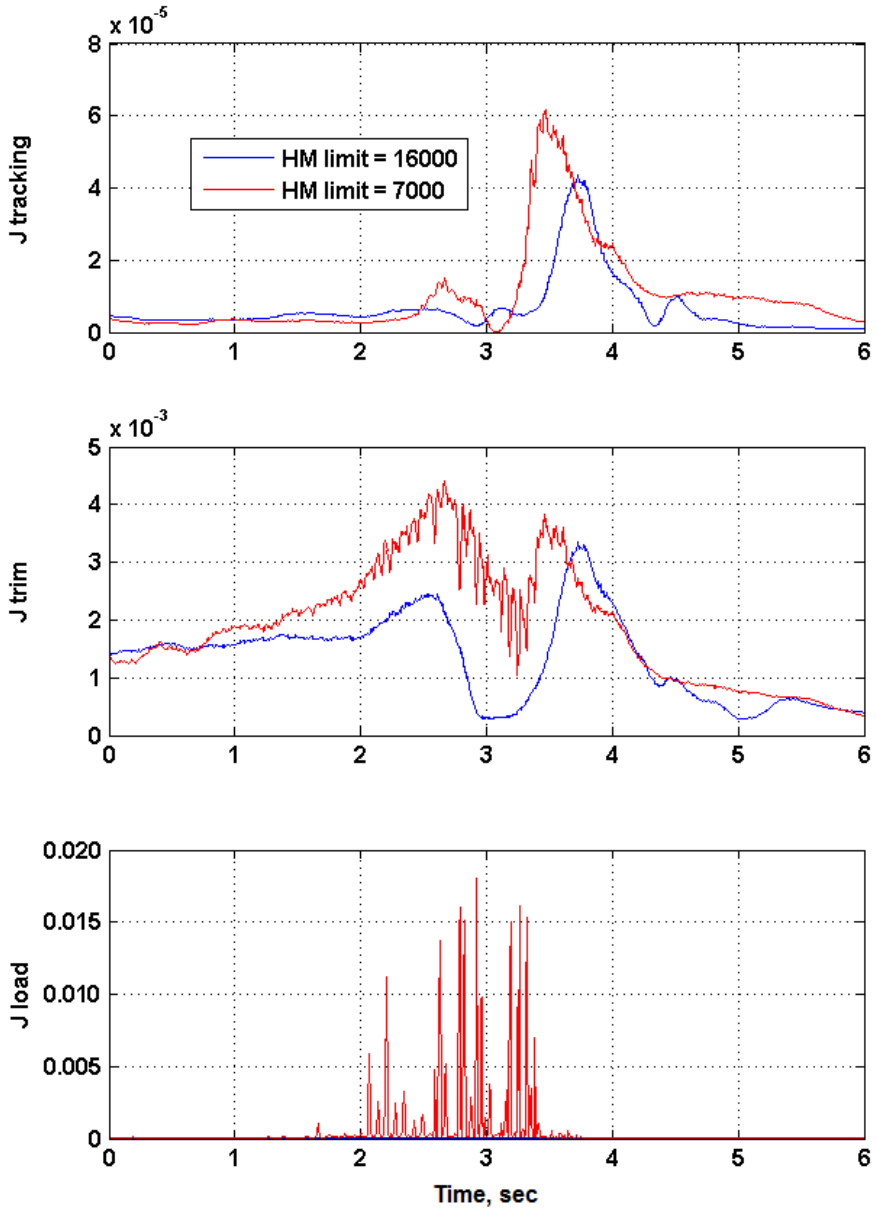

Figure 11. Individual contributions to the cost function during a 2.5-g level turn (FC6).

The performance of the OCLA experiment at a slower airspeed (FC11) is shown in Fig. 12 through Fig. 14. Only the performance for the level turn is shown because the roll performance at FC11 is similar to FC6, suggesting that the roll performance is not affected significantly by airspeed. However, the lower airspeed appears to adversely affect the performance of the control laws during the level turn. The structural oscillations at FC11, shown in Fig. 12, are more pronounced than for the same maneuver at FC6. Additionally, based on the number of iterations used by the optimizer it appears obtaining good convergence is more challenging at FC11. This degradation in performance at lower speed for elevated g maneuvers is important for understanding the handling qualities results in section C.

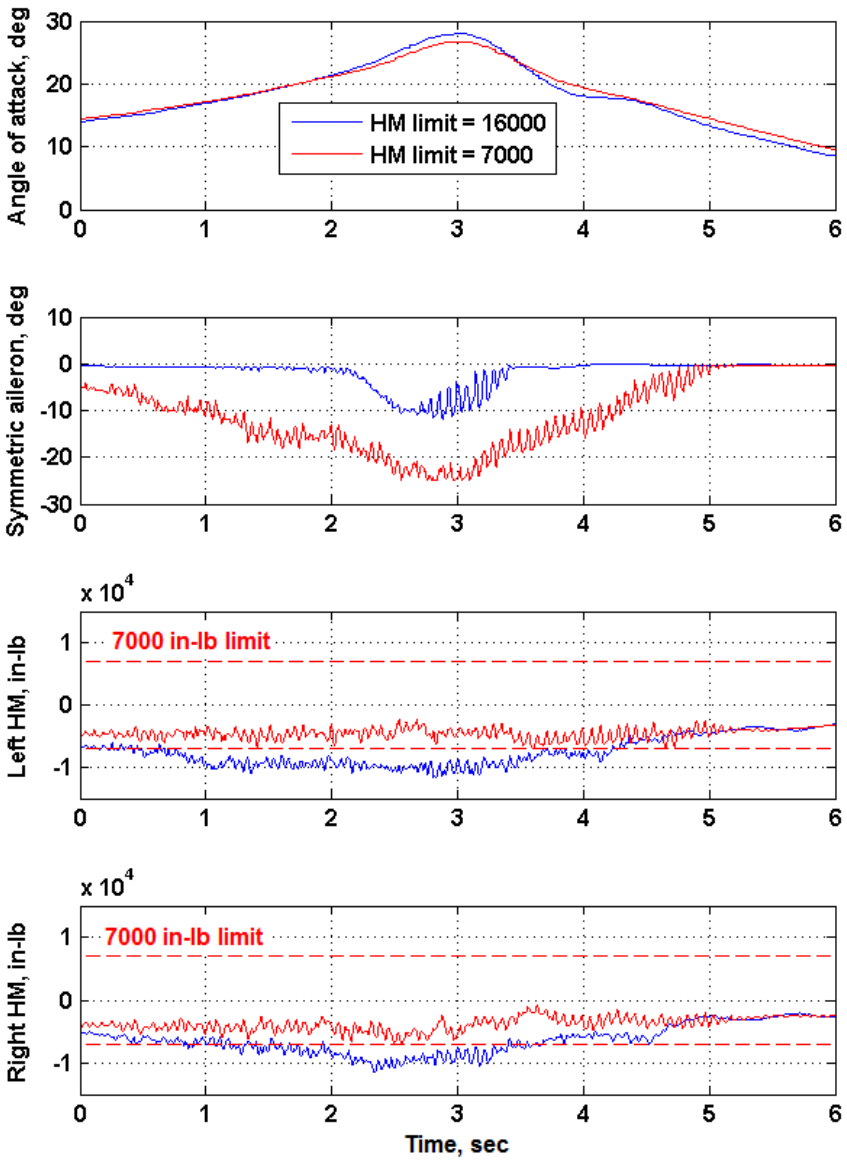

Figure 12. Performance during a 2.5-g level turn (FC11).

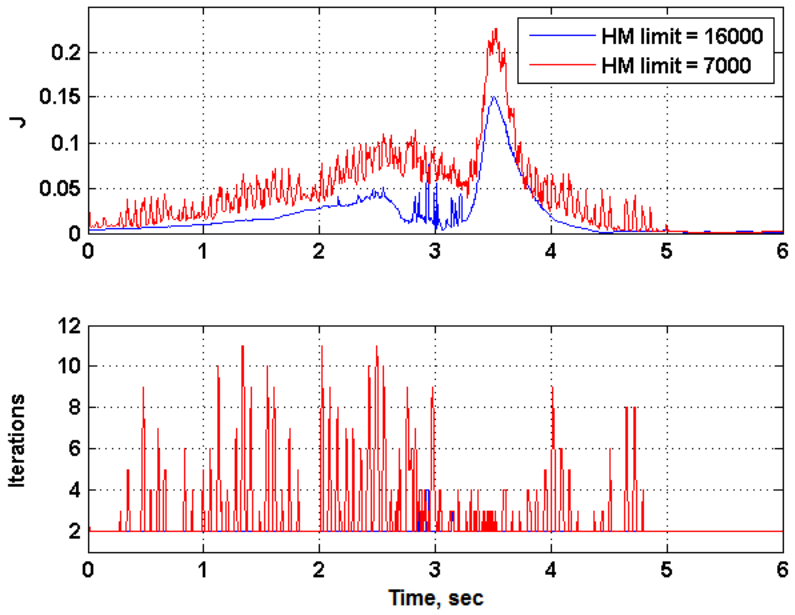

Figure 13. Cost and number of iterations during a 2.5-g level turn (FC11).

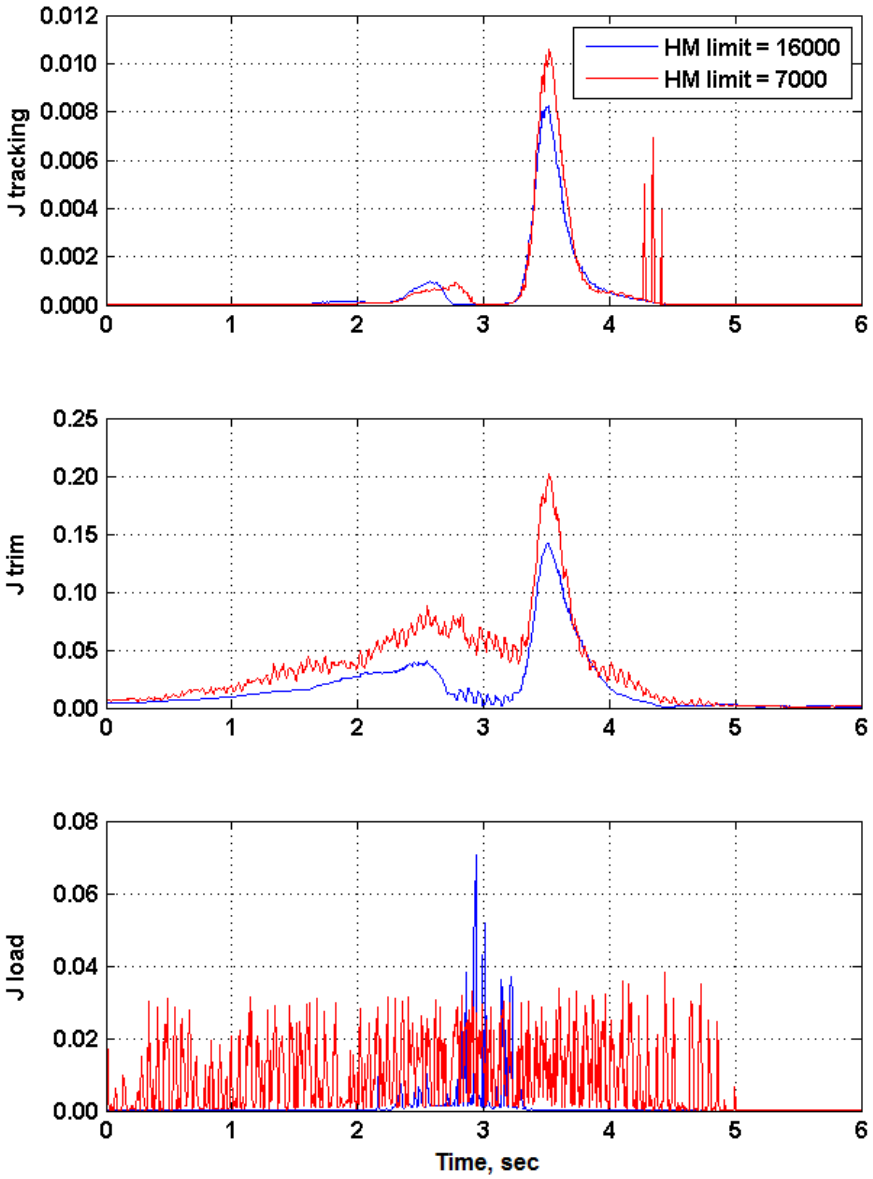

Figure 14. Individual contributions to the cost function during a 2.5-g level turn (FC11).

B. Effect of OCLA on Control Response (Objective 2)

Lower Order Equivalent Systems (LOES) analysis can be a valuable tool for gaining insight into a complex system. Even highly nonlinear systems can often be accurately represented by LOES (Ref. 10). Figure 15 illustrates how a LOES representation of the OCLA roll mode depends on the cost function parameters. It can be seen that the roll mode gain (K) decreases slightly with decreasing hinge-moment limit. This reduction in roll mode gain intuitively makes sense because less aileron command allowable translates to reduced roll moment that can be generated. Steeper load constraints (higher n) can be seen to lessen this effect and preserve roll authority up to the most restrictive hinge-moment limits. The roll mode time constant ($\mathbf{1}/\boldsymbol{\omega_n}$) exhibits a similar behavior. The time constant increases with decreasing hinge moment allowable for the same reason; less aileron command allowable translates to reduced roll bandwidth. Again steeper load constraints (higher n) preserve more roll authority even with restrictive load limits. There are no significant trends that affect the perceived roll response for the damping ratio.

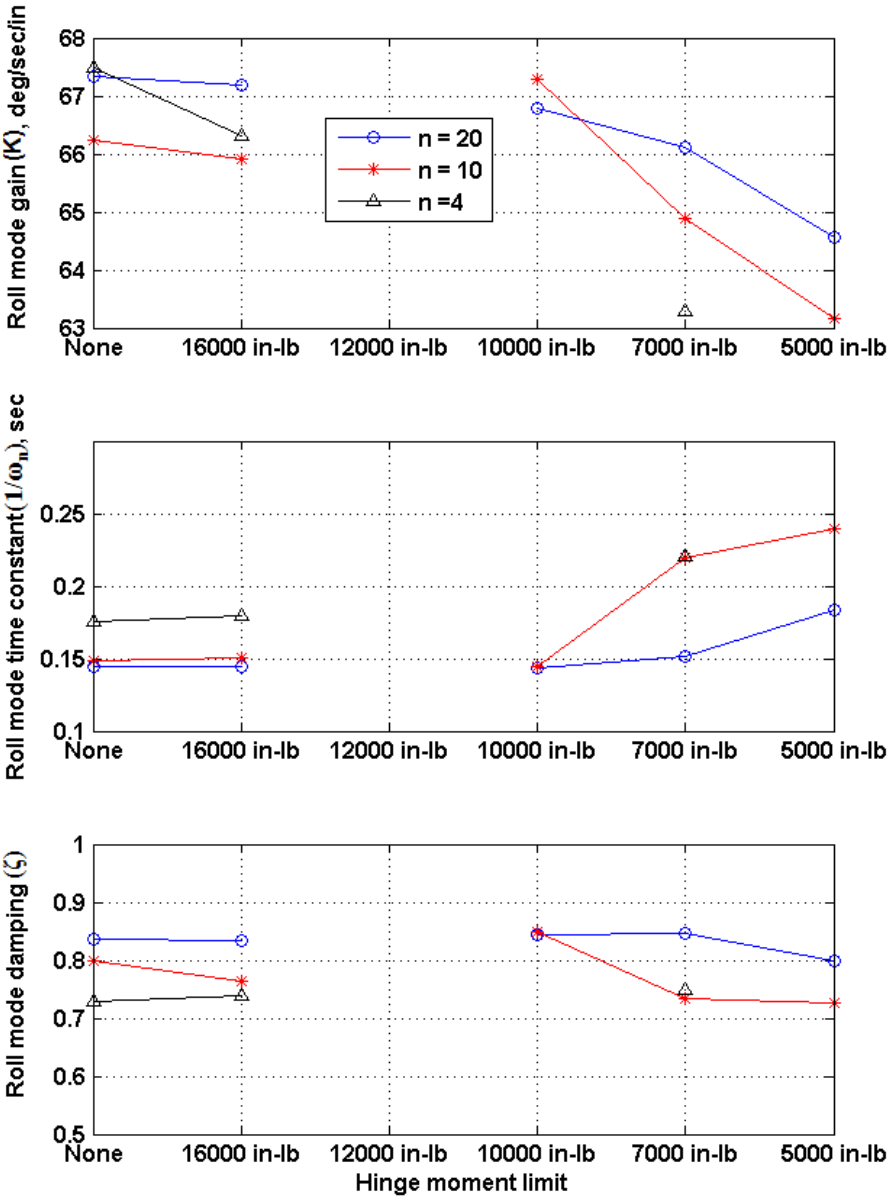

Figure 15. Low order equivalent systems $\frac{p}{dap} = \frac{K\omega_n^2 e^{-0.08s}}{s^2+2\zeta\omega_n s+\omega_n^2}$ parameter variation for control architecture.

C. Effect of OCLA on Piloted Handling Qualities (Objective 3)

One very important aspect of any load limiting control law is that it must be able to provide adequate control characteristics to the pilot. If the pilot and aircraft cannot complete the desired mission due to reductions in performance, due to the load limiting algorithm, then very little has been gained. The 2-g air-to-air tracking task was used to evaluate the OCLA algorithm with an operationally relevant and challenging task for the vehicle. Tables 4 and 5 show all of the Cooper-Harper[7] handling qualities ratings for all of the configurations tested in flight. Each of the three pilots rated the baseline controller, and the OCLA controller. Pilot A only flew the handling qualities maneuvers at the end of the flight at a light aircraft weight. Pilots B and C flew the handling qualities maneuvers at multiple weights.

The gross acquisition task (Table 4) shows that the OCLA controller gets mostly level 1 handling ratings (1-3). These ratings do not appear to depend significantly on the load limiting level and are very similar to those given to the baseline aircraft control system. It can be concluded that for the gross acquisition task that the OCLA controller with load limiting meets or exceeds the desired performance objectives.

It was expected that the handling qualities would be degraded with more restrictive limits due to more sluggish roll responses, and that trend does appear in the ratings for the Fine Tracking task in Table 5 and Fig. 16. Additionally the ratings appear to show a degradation in handling qualities as a function of vehicle weight. This weight dependency was unexpected as the OCLA control system was designed to account for the weight variation via the dynamic inversion to produce pitch, roll, and yaw characteristics that are consistent across the test envelope. The pilots also commented that the fine tracking task was more difficult at the end of the maneuver than at the beginning for all weights. The pilots consistently highlighted deficiencies in pitch that were producing undesired oscillations at the end of each fine tracking maneuver. Figure 17 illustrates how the pitch task evolved during the fine tracking task. As the task progressed, airspeed bled off resulting in increased angle of attack, especially for the heaviest weights. Angle of attack is a primary driver for aileron hinge moment, along with aileron deflection. At the higher angles of attack and more restrictive limits, it can be seen in Fig. 17 that the OCLA controller has to retract the ailerons in order to alleviate load, thus resulting in further increases in angle of attack. The higher angles of attack resulted in trim configurations with less desirable properties and more difficulty performing the fine tracking task. The poorly trimmed aircraft did not have the performance to complete the task within the desirable criteria for the fine tracking task, and the pilots rated the system accordingly. Overall for both gross acquisition and fine tracking, the ratings suggest that the OCLA controller exhibited at least adequate handling qualities, and that for many of the conditions produced equally good handling qualities when compared to the baseline controller.

Table 4. Cooper-Harper ratings for gross acquisition task.

Gross acquisition	Baseline	16000 in-lb	7000 in-lb	5000 in-lb
Pilot A heavy weight				
Pilot A middle weight				
Pilot A light weight	3	3	3	3
Pilot B heavy weight	5	3	4	5
Pilot B middle weight				
Pilot B light weight	3		2	3
Pilot C heavy weight	2	3	2	2
Pilot C middle weight	2		2	2
Pilot C light weight			2	

Table 5. Cooper-Harper ratings for fine tracking task.

Fine tracking	Baseline	16000 in-lb	7000 in-lb	5000 in-lb
Pilot A heavy weight				
Pilot A middle weight				
Pilot A light weight	4	3	4	5
Pilot B heavy weight	3	3	5	4
Pilot B middle weight				
Pilot B light weight	3		4	2
Pilot C heavy weight	3	5	6	6
Pilot C middle weight	3		5	6
Pilot C light weight			4	

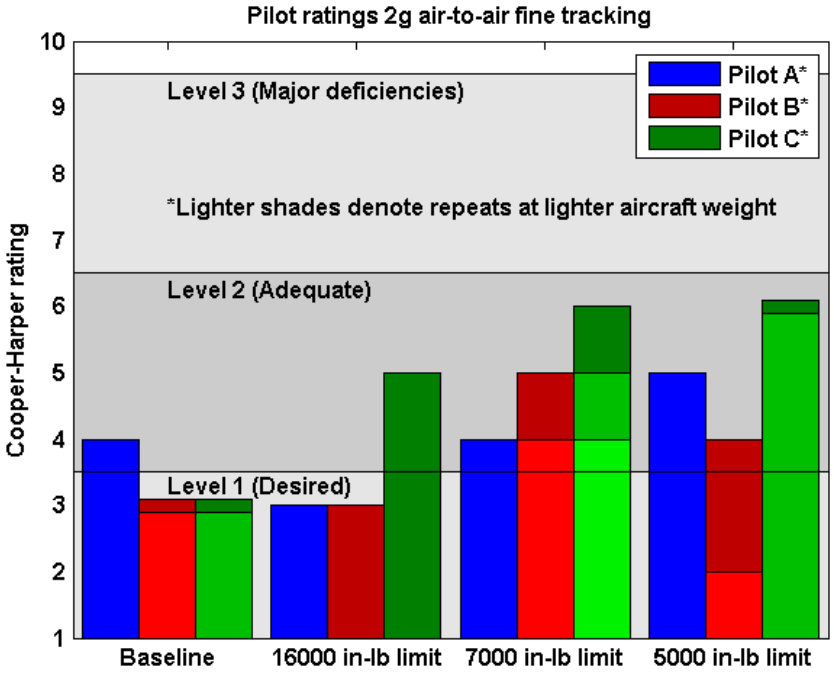

Figure 16. Pilot Cooper-Harper ratings comparisons.

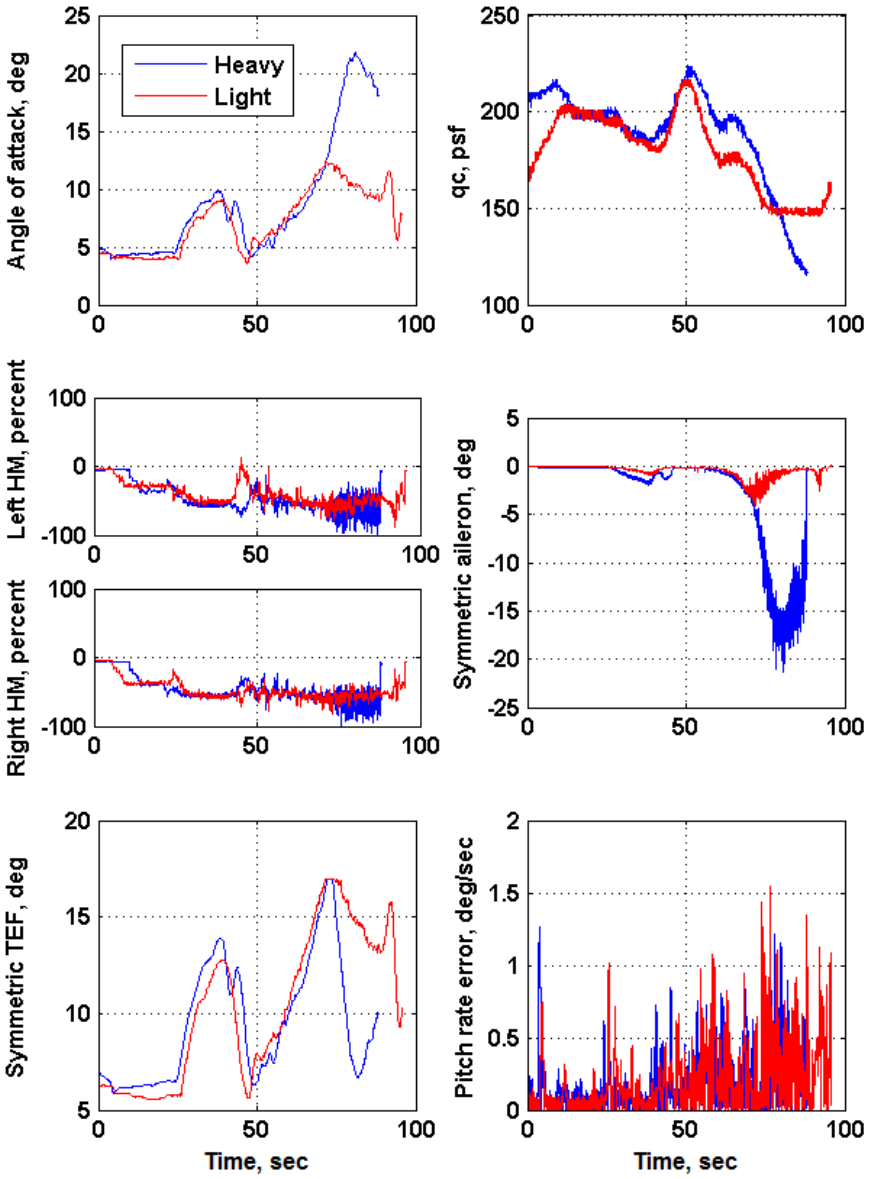

Figure 17. Comparison of the tracking task heavy versus light for Pilot C with 7000 in-lb limit.

D. Structural Modal Interactions (SMI) Considerations

One large area of uncertainty going into the flights was whether the OCLA architecture would exhibit classical SMI behaviors and if those properties could be predicted, analyzed, and mitigated with conventional modal filtering. However, good models of the dynamic response of the hinge-moment measurement and the vehicle structural modes did not exist prior to flight. Therefore, two test configurations were included in the flight software to explore these properties; one with no SMI filtering, and a second with a first order low pass filter at 5 Hz on the aileron hinge-moment feedback signals. Figure 18 shows the loop that is of concern, and Fig. 19 shows the theoretical OCLA strain to aileron command feedback gain as a function of measure load. For more details on the loop gain and how to derive it see Ref. 9. Figure 20 shows the measured open loop frequency response of the loop in Fig. 18. It should be noted that the data to generate the open loop frequency response in Fig. 20 was not available prior to the OCLA flights. If the data used to generate Fig. 20 had been available prior to the flights it would have been used to design notch filters

on the strain-feedback signals to prevent undesirable SMI. The -180° phase crossover frequency in Fig. 20 occurs at roughly 20 Hz, suggesting that if a control configuration with sufficient gain at 20 Hz is engaged a 20 Hz SMI instability will exist. Based on the gain estimate in Fig. 20 the unfiltered configuration should exhibit an SMI at 20 Hz because the magnitude is just above 0 db. Scaled up accelerometer data in Fig. 20 are included to show the frequencies at which the wing structure resonates. There are a number of peaks in the accelerometer frequency response that do not show up in the control response, suggesting that the control response to this modal content is stable. However, the accelerometer data show the same peak at 20 Hz that is apparent in the strain data and the control response. The fact that the accelerometer frequency response has a peak at 20 Hz suggests that this mode is a genuine SMI and not just a controller/actuator mode. Figures 21 and 22 show where the actual SMI instability was observed in flight. Figure 21 shows that the instability arises at 20 Hz as predicted by the analysis of Fig. 20. Figure 22 shows that the instability results in a bounded limit cycle oscillation. This result suggests that SMIs related to OCLA can be gain stabilized with traditional notch filtering and that traditional analysis approaches can be used. The effect of SMI instability is bounded due to both the low dynamic pressure and aileron rate limiting which made it safe to explore in flight.

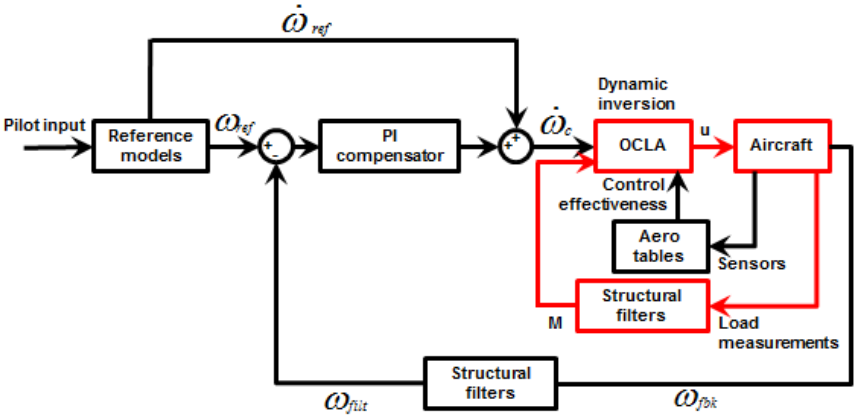

Figure 18. Hinge-moment feedback loop.

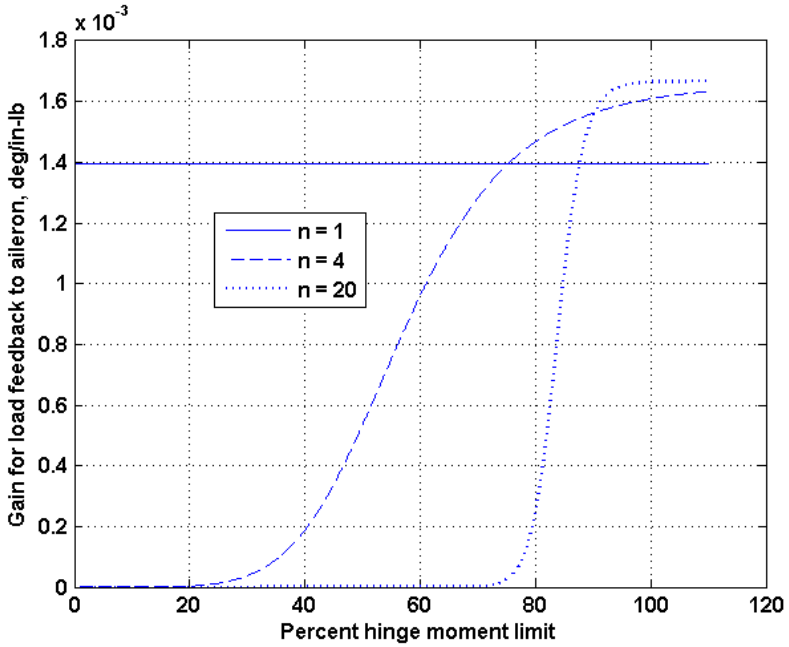

Figure 19. Aileron hinge-moment loop gain illustration.

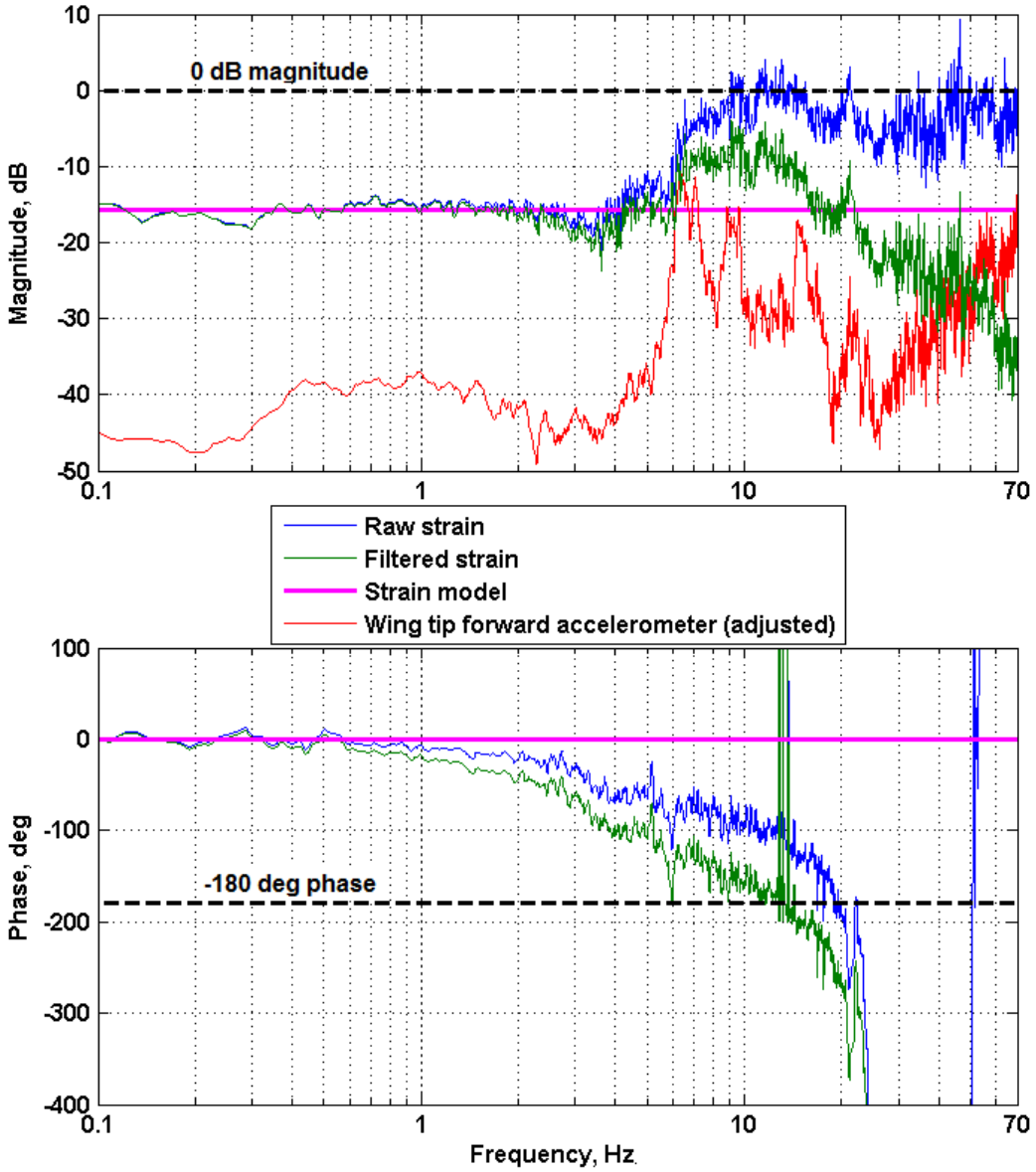

Figure 20. Open loop frequency response of the aileron hinge-moment feedback loop (n=4, HM limit = 10000, N=0.45, FC 6).

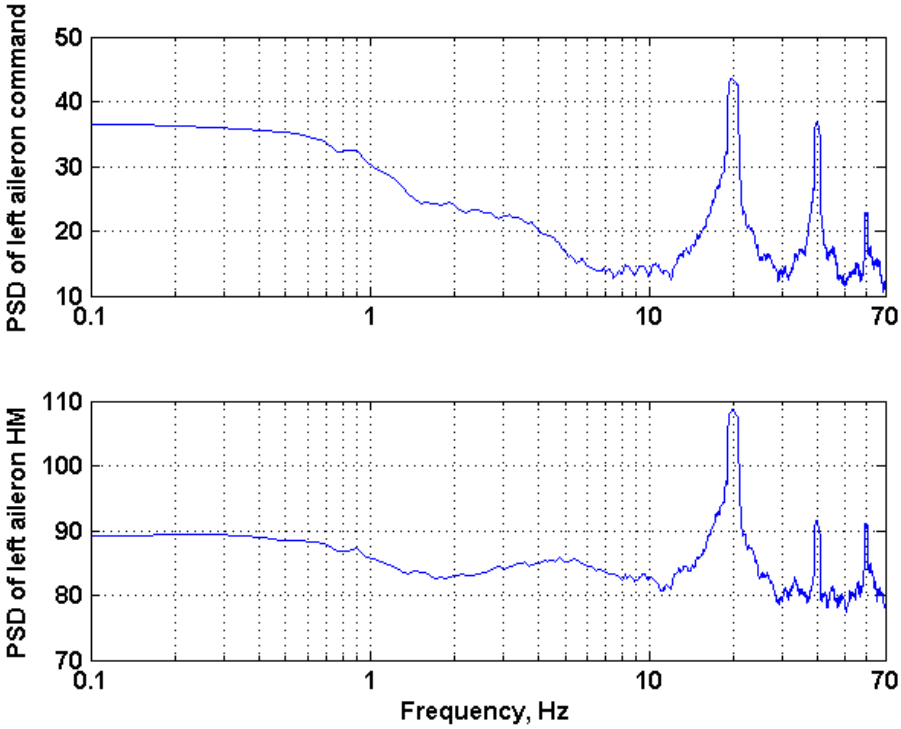

Figure 21. PSD of aileron command and aileron hinge moment during unstable SMI excitation (n = 4, HM limit = 10000, FC6).

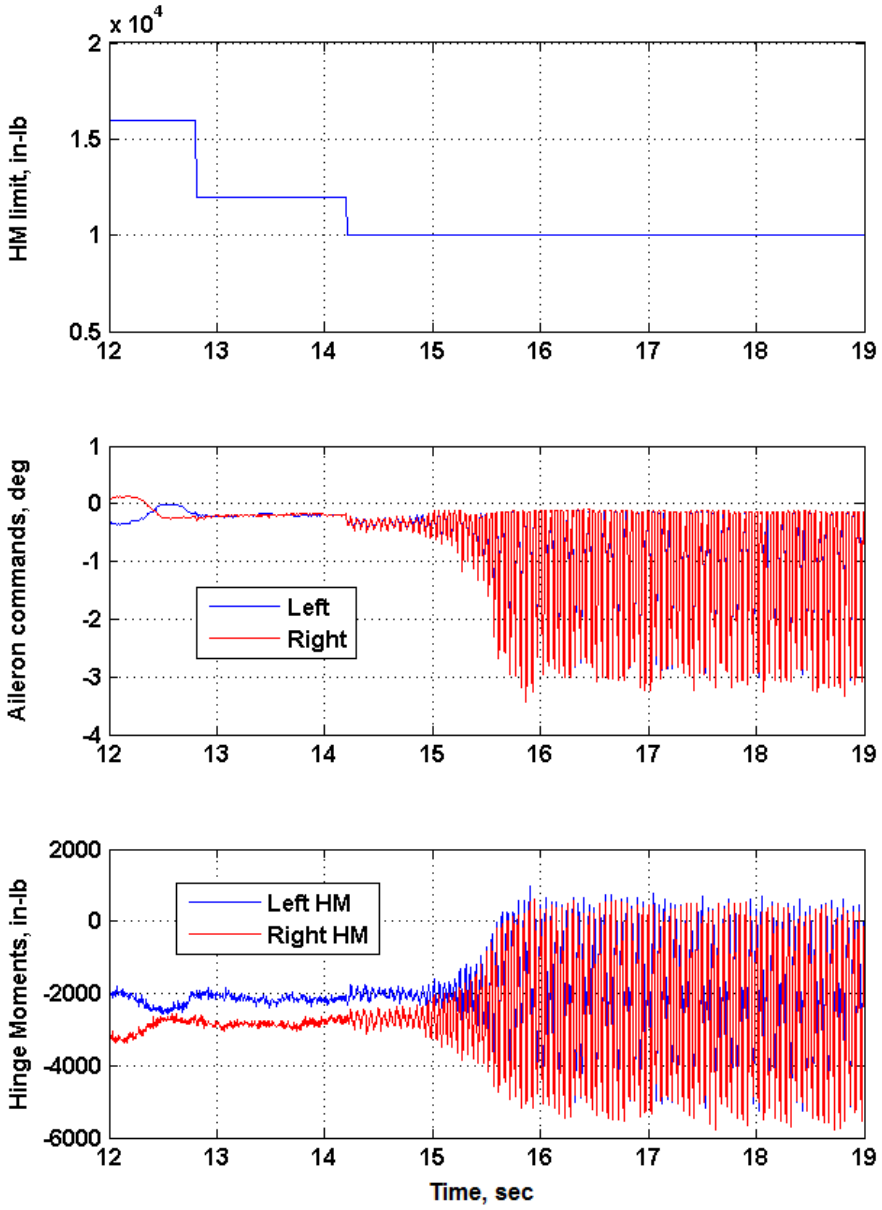

Figure 22. Time domain response during unstable SMI excitation (n=4, HM limit = 10000, FC6).

VIII. Conclusions

The flight results for the Optimal Control and Load Allocation (OCLA) experiment suggest a number of important conclusions. Overall the experiment met all of the objectives: limit aileron hinge moment, preserve roll performance, and maintain desirable handling qualities. The aileron hinge moments were limited to below the specified limit 100% of the time, and the algorithm provided the same level of overload protection for both roll and elevated g pitch maneuvers. OCLA preserved the attainable roll rate for the aircraft by redistributing roll control commands to the trailing-edge flaps and stabilators and away from the ailerons as they approached the load limits. The steep load constraints allowed roll performance to be maintained at both low and high speed flight conditions for all but the most restrictive hinge-moment limits. Adequate handling qualities were obtained for all of the configurations tested, with level 1 handling qualities for the gross acquisition task and for the fine tracking task at light aircraft weight. The flight-

test results showed that traditional structural modal interaction (SMI) analysis and mitigation techniques can be applied to the OCLA approach. The algorithm exhibited excellent convergence properties even for the most nonlinear load constraints.

A number of issues were uncovered during the flight-test activities that suggest some areas where further research and development is merited. A number of handling qualities deficiencies were observed at elevated g due to early activation of the load constraint during elevated g pitch maneuvers. This issue was the most pronounced at low airspeed. This result suggests the need for further shaping of the individual load feedback signals.

References

[1]Frost, S. A., et al., "Application of Structural Load Feedback in Flight Control," AIAA-2011-6288, 2011.

[2]Bodson, M., and Frost, S. A., "Load Balancing Control Allocation," *Journal of Guidance, Control, and Dynamics*, Vol. 34 No. 2, March-April 2011.

[3]Bodson, M., "Evaluation of Optimization Methods for Control Allocation," *Journal of Guidance, Control, and Dynamics*, Vol. 25, No. 4, July-August 2002.

[4]National Transportation Safety Board Aircraft Accident Report, "In-Flight Separation of Vertical Stabilizer American Airlines Flight 587 Airbus Industrie A300-605R, N14053 Belle Harbor, New York November 12, 2001," NTSB/AAR-04/04 PB2004-910404 Notation 7439B, 2004.

[5]Miller, C. "Nonlinear Dynamic Inversion Baseline Control Law: Architecture and Performance Predictions," AIAA 2011-6467, 2011.

[6]Miller, C. "Nonlinear Dynamic Inversion Baseline Control Law: Nonlinear Dynamic Inversion Baseline Control Law: Flight-Test Results for the Full-scale Advanced Systems Testbed F/A-18 Airplane," AIAA 2011-6468, 2011.

[7]Cooper, G. E., [and] Harper, Jr., R. P., "The use of Pilot Rating in the Evaluation of Aircraft Handling Qualities," NASA TN D-5153, 1969.

[8]Pavlock, K., "Full-Scale Advanced Systems Testbed: Ensuring Success of Adaptive Control Research Through Project Lifecycle Risk Mitigation," *Society of Flight Test Engineers*, SFTE 2011 42-12, 2011.

[9]Miller, C. J., and Goodrick, D., "Optimal Control Allocation with Load Sensor Feedback for Active Load Suppression, Experiment Development," AIAA 2016-#### (to be published), 2017.

[10]Hodgkinson, J., and LaManna, W. J., "Equivalent System Approaches to Handling Qualities Analysis and Design Problems of Augmented Aircraft," AIAA-1977-1122, 1977.